

**Technical Support Document
for the Final
Clean Air Mercury Rule**

Air Quality Modeling

**U.S. Environmental Protection Agency
Office of Air Quality Planning and Standards
Research Triangle Park, NC 27711**

March 2005

Table of Contents

I.	Introduction.....	2
II.	Emission Inventories and Estimated Emissions Reductions.....	3
III.	Model, Domain, Configuration, Inputs, and Application.....	7
IV.	CMAQ Model Performance Evaluation.....	12
V.	Impacts of CAMR on Mercury Deposition.....	16
VI.	Summary of Findings: HUC Level Deposition analysis.....	19
VII.	References.....	22

I. Introduction

This section summarizes the emissions inventories and air quality modeling that serve as the inputs to the benefits analysis for the Clean Air Mercury Rule (CAMR). EPA used a sophisticated photochemical air quality model to predict the levels of mercury deposition for a 2001 base year and a 2020 baseline reflecting co-control of mercury from implementation of the Clean Air Interstate Rule (CAIR) as well as two control options for CAMR. The estimated changes in mercury deposition associated with the control options were then combined with fish tissue data for use in estimating health and welfare effects. In addition, utility attributable deposition of mercury was estimated based on zero-out modeling for both the 2001 and 2020 baselines.

The 1997 Mercury Study Report to Congress noted that “a single air quality model which was capable of model both the local as well as regional fate of mercury was not identified.” In fact, at that time such a model did not exist. Thus, the modeling approach for this report employed two models: 1) the Regional Lagrangian Model of Air Pollution (RELMAP) to address regional-scale atmospheric transport, and 2) the Industrial Source Code model (ISC3) to address local-scale analyses (i.e., within 50 km of source). This approach also required assumptions to be made about the background concentrations of mercury that were uniformly added to the regional component and the use of “model plants” to represent typical sources for the local-scale transport. At this time, the Agency would have significant concerns about using the ISC3 model for assessments of Hg deposition associated with CAMR. The Agency will later this year promulgate the American Meteorological Society/Environmental Protection Agency Regulatory Model (AERMOD) that will replace ISC3 as the recommended and preferred model for use in regulatory permit modeling assessments. This model contains the Argonne National Laboratory (ANL) versions of the wet and dry deposition algorithm which contain refinements beyond the ISC3 model and are considered more robust through extensive testing and evaluation. The ISC3 outputs for wet and dry deposition were never fully tested and verified for use in regulatory applications.

The Agency views the application of a more robust and sophisticated modeling approach as critical and required for assessing the mercury deposition associated with CAMR because of the density and properties of mercury and its complex transport and reactions in the atmosphere. The Community Multiscale Air Quality (CMAQ) modeling system best meets our requirements and the recommendations of the Report to Congress for a ‘single air quality model’ to address mercury deposition. CMAQ is a three-dimensional grid-based Eulerian air quality model designed to estimate pollutant concentrations and depositions over large spatial scales (e.g., over the contiguous United States). Because it accounts for spatial and temporal variations as well as differences in the reactivity of mercury emissions, CMAQ is the best available model for evaluating the impacts of the CAMR on U.S. mercury depositions. This model appropriately accounts for the atmospheric reactions of specific mercury emissions and their significance in the levels of deposition as shown through our results here for CAMR. In addition, the boundary and initial species concentrations are provided by a three-dimensional global atmospheric chemistry and transport model, i.e., Harvard’s GEOS-CHEM model. The model simulations are performed based on plant-specific emissions of mercury by species as provided by the Integrated

Planning Model (IPM).

Section II provides a summary of the emissions inventories that were modeled for this rule. Section III discusses the model, domain, configuration, inputs, and application. Section IV summarizes the model performance. Section V summarizes the results of estimating mercury depositions for the 2001 and 2020 scenarios modeled. Section VI summarizes the deposition findings at water bodies for the scenarios modeled and Section VII provides the references for this analysis.

II. Emissions Inventories and Estimated Emissions Reductions

This section summarizes the emissions inventories that serve as the inputs to the air quality model used for the Clean Air Mercury Rule (CAMR). The CAMR Emissions Inventory Technical Support Document (TSD) discusses the development of the 2001 and 2020 emissions inventories for input to the air quality modeling of this final rule in greater detail (EPA, 2005a). Table 1 provides the emission sources and the basis for current and future-year inventories, while Table 2 summarizes the mercury emissions by species from utilities, also known as Electric Generating Units (EGUs), and other sources that were used in modeling of mercury deposition.

As Table 2 demonstrates, a total of almost 115 tons of mercury were emitted across all sources in 2001. EGUs emitted a total of 48.6 tons, or 42.3 percent of mercury emissions across all sources during this base year. Almost 21 tons of the most readily deposited form of mercury, i.e., reactive gaseous mercury (RGM), were emitted by these utilities and therefore comprised 42.4 percent of their mercury emissions.

The 2020 baseline emissions shown in Table 2 accounts for increases in economic activity and population growth between 2001 and 2020 that lead to increased production in the utility and manufacturing sectors and hence increases in emissions over time, as well as the implementation of regulatory policies from MACT standards (primarily on non-EGU sources) and the CAR controls (as applied to EGUs in the eastern U.S.) which decreases emissions over this time period. Total mercury emissions in 2020 are roughly 87 tons, reflecting a net reduction of almost 28 tons (or 24 percent) from 2001 levels. As shown, the 2020 baseline with CAR shows net reductions in mercury emissions for EGUs of 14.2 tons or a 29.1 percent reduction from 2001 levels. Utility emissions are expected to account for 39.5 percent of total mercury emissions in 2020, which is only slightly lower than their share in 2001. However, the reductions associated with CAR co-control show a large reduction of 61.8 percent in their emissions of reactive gaseous mercury relative to their 2001 level of emissions, i.e., 20.58 tons in 2001 to only 7.87 tons in 2020.

Table 3 shows the reductions in mercury emissions associated with the CAMR Control Option 1 in 2020. The 2020 EGU emissions are reduced by approximately 10 tons to a total of 25 tons, representing a 11 percent reduction from total baseline emissions in 2020 (with CAR), or a 27 percent reduction from the EGU sector alone. Under CAMR Control Option 2, EGU emissions are further reduced by an additional 4 tons to a total of roughly 21 tons. This

represents a 16 percent reduction from total emissions from the 2020 baseline (with CAR), or a 39 percent reduction from the EGU sector alone.

In comparison to current mercury emissions (i.e., the 2001 base year scenario), the CAR and CAMR Option 1 achieve a total reduction in EGU emissions of approximately 24 tons (48 percent), while CAR and CAMR Option 2 achieve a total reduction in EGU emissions of approximately 28 tons (57 percent).

Table 1. Summary of Emissions Sources for 2001 and 2020 Mercury Emissions Inventories

Sector	Emissions Source	2001 Base Year	2020 Base Case Projections
Utilities - Electric Generating Units (EGU)	Power industry electric generating units (EGUs)	1999 National Emission Inventory (NEI) data	Integrated Planning Model (IPM) reflecting growth in Btu demand as well as regulatory policies implemented through 2020, such as the Clean Air Interstate Rule
Non-EGU point sources	Non-Utility Point	1999 NEI, with medical waste incinerator sources replaced with draft 2002 NEI	(1) Department of Energy (DOE) fuel use projections, (2) Regional Economic Model, Inc. (REMI) Policy Insight® model, (3) decreases to REMI results based on trade associations, Bureau of Labor Statistics (BLS) projections and Bureau of Economic Analysis (BEA) historical growth from 1987 to 2002, (4) Maximum Achievable Control Technology category growth and control assumptions
Non-point sources	All other stationary sources inventoried at the county level	1999 NEI, with medical waste incinerator sources replaced with draft 2002 NEI	same as above

^aThis table documents only the sources of data for the U.S. inventory. The sources of data used for Canada and Mexico are explained in the technical support memorandum and were held constant from the base year to the future years.

Table 2. Summary of Mercury Emissions by Species: 2001 and 2020 (with CAR) Baselines

Emissions Source	Mercury Emissions Species (tons)			Total Mercury Emissions (tons)
	Elemental	Reactive Gaseous	Particulate	
<i>2001 Base Year</i>				
EGUs	26.26	20.58	1.73	48.57
Non-EGU Point	37.85	13.33	7.60	58.78
Non-point	5.05	1.53	0.96	7.54
Total, All Sources	69.16	35.44	10.29	114.89
<i>2020 (with CAR) Baseline</i>				
EGUs	25.72	7.87	0.83	34.42
Non-EGU Point	28.03	10.37	6.61	45.01
Non-point	5.69	1.30	0.77	7.76
Total, All Sources	59.44	19.54	8.21	87.19

Table 3. Summary of Changes in Mercury Emissions Associated with CAMR Control Option 1: 2020

Emissions Source	Change in Mercury Emissions Species (tons)			Total Change in Mercury Emissions (tons)
	Elemental	Reactive Gaseous	Particulate	
EGUs	8.07 (31.4%)	1.30 (16.5%)	0.00 (0.0%)	9.37 (27.2%)
Non-EGU Point	n/a	n/a	n/a	n/a
Non-point	n/a	n/a	n/a	n/a
Total, All Sources	8.07 (13.6%)	1.30 (6.7%)	0.00 (0.0%)	9.37 (10.7%)

Note: n/a is not applicable.

Table 4. Summary of Changes in Mercury Emissions Associated with Control Option 2: 2020

Emissions Source	Change in Mercury Emissions Species (tons)			Total Change in Mercury Emissions (tons)
	Elemental	Reactive Gaseous	Particulate	
EGUs	11.39 (44.3%)	2.16 (27.4%)	0.04 (4.8%)	13.59 (39.5%)
Non-EGU Point	n/a	n/a	n/a	n/a
Non-point	n/a	n/a	n/a	n/a
Total, All Sources	11.39 (19.2%)	2.16 (11.1%)	0.04 (0.5%)	13.59 (15.6%)

Note: n/a is not applicable.

III. Model, Domain, Configuration, Inputs, and Application

Air quality modeling for mercury deposition was conducted using the Community Multiscale Air Quality Model (CMAQ). The CMAQ modeling system is a comprehensive three-dimensional grid-based Eulerian air quality model designed to estimate pollutant concentrations and depositions over large spatial scales (Dennis et al., 1996; Byun and Ching, 1999; Byun and Schere, 2004). The CMAQ model is a publically available, peer-reviewed, state-of-the-science model consisting of a number of science attributes that are critical for simulating the oxidant precursors and non-linear chemical relationships associated with the formation of mercury. Version 4.3 of CMAQ (Byun and Schere, 2004, Bullock and Brehme, 2002) was used for CAMR. This version reflects updates to earlier versions in a number of areas to improve the underlying science and address comments from peer review. The updates in mercury chemistry used for CAMR from that described in (Bullock and Brehme 2002) are as follows: (1) the elemental mercury (Hg0) reaction with H₂O₂ assumes the formation of 100 percent reactive gaseous mercury (RGM) rather than 100 percent particulate mercury (HgP), (2) the Hg0 reaction with ozone assumes the formation of 50 percent RGM and 50 percent HgP rather than 100 percent HgP, (3) the Hg0 reaction with OH assumes the formation of 50 percent RGM and 50 percent HgP rather than 100 percent HgP, and (4) the rate constant for the Hg0 + OH reaction was lowered from 8.7 to 7.7 x10⁻¹⁴cm³molecules⁻¹s⁻¹. CMAQ simulates every hour of every day of the year and requires a variety of input files that contain information pertaining to the modeling domain and simulation period. These include hourly emissions estimates and meteorological data in every grid cell as well as a set of pollutant concentrations to initialize the model and to specify concentrations along the modeling domain boundaries. These initial and boundary concentrations were obtained from output of a global chemistry model. We use the model predictions in a relative sense by first determining the ratio of mercury deposition predictions. The calculated relative change is then combined with the corresponding fish tissue concentration data to project fish tissue concentrations for the future case scenarios. The following sections provide a more detailed discussion of the modeling and a summary of the results. Key science aspects of CMAQ as applied for CAMR include:

- Gas-Phase Chemical Solver: Euler Backward Iterative (EBI) scheme
- Advection Scheme (vertical and horizontal): Piecewise Parabolic Method (PPM) scheme
- Vertical Diffusion: K-theory eddy diffusivity scheme; minimum diffusivity is 1 m²/sec
- Dry Deposition: M3DRY module, modified RADM scheme with Pleim-Xiu land surface model
- Aqueous Chemistry: RADM Bulk scheme
- Cloud Scheme: RADM Cloud scheme
- Vertical Coordinate: Terrain-following Sigma coordinate

A. CMAQ Modeling Domain and Configuration

As shown below in Figure 1, the CMAQ modeling domain encompasses all of the lower 48 States and extends from 126 degrees west longitude to 66 degrees west longitude and from 24 degrees north latitude to 52 degrees north latitude. The modeling domain is segmented into rectangular blocks referred to as grid squares. The model predicts pollutant concentrations and depositions for each of these grid cells. For this application the horizontal domain consisted of 16,576 grid cells that are roughly 36 km by 36 km. The modeling domain contains 14 vertical layers with the top of the modeling domain at about 16,200 meters, or 100 millibar. The vertical layer structure for CMAQ used for the CAMR applications is shown in Table 5 (this table can be found below, in the section C.). The height of the surface layer is 38 meters.

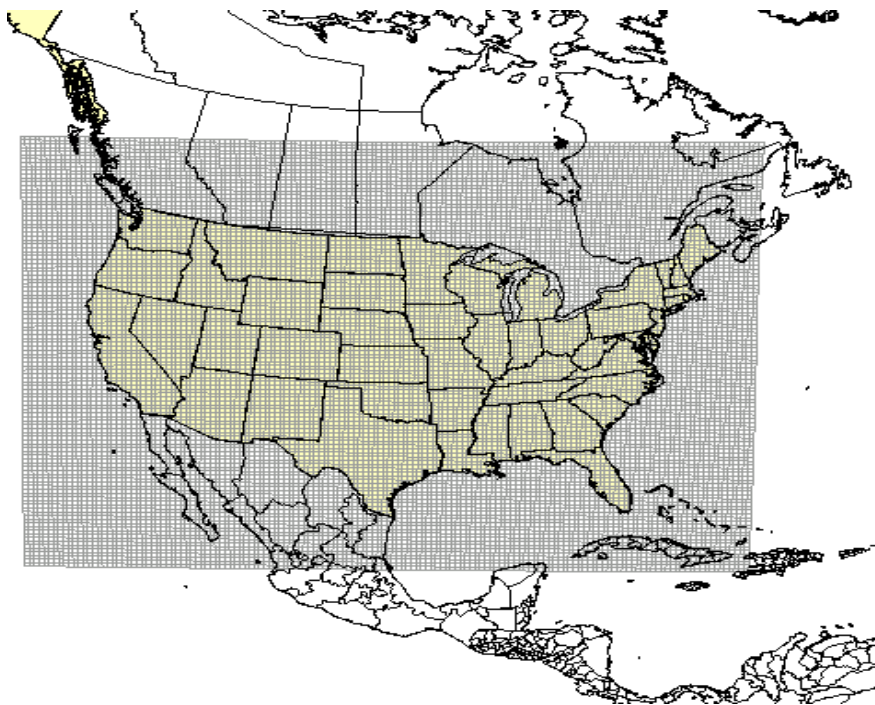


Figure 1. CMAQ Modeling Domain

B. Time Period Modeled For Mercury Deposition

CMAQ was run for a full year for each of the six CAMR emissions scenarios modeled. The overall model run time for completing an annual simulation was reduced by dividing the year into two six-month periods which were run in parallel on different computer processors. That is, the annual simulation was performed as two separate six month model runs. One run was for January through June and the other run was for July through December. Each six-month runs included a 10-day ramp-up (i.e., “spin-up”) period designed to minimize the influence of the initial concentration fields (i.e., initial conditions) used at the start of the model run. The development of initial condition concentrations is described in Section D, below. The ramp-up periods used for the CAMR CMAQ applications are as follows:

- first six-month ramp-up period is December 22 - 31, 2000
- second six-month ramp-up period is June 21 - 30, 2001

Model predictions from these ramp-up periods were disCAIRded and not used in analyses of the modeling results. The meteorological conditions, initial conditions and boundary conditions were held constant for each of the emissions scenarios modeled and are described below in sections C and D.

C. Meteorological Inputs to CMAQ

Meteorological data, such as temperature, wind, stability parameters, and atmospheric moisture contents influence the formation, transport, and removal of air pollution. The CMAQ model requires a specific suite of meteorological input files in order to simulate these physical and chemical processes. For the CAMR CMAQ modeling, meteorological input files were derived from a simulation of the Pennsylvania State University / National Center for Atmospheric Research Mesoscale Model (Grell et al., 1994) for the entire year of 2001. This model, commonly referred to as MM5, is a limited-area, nonhydrostatic, terrain-following system that solves for the full set of physical and thermodynamic equations which govern atmospheric motions. For this analysis, version 3.6.1 of MM5 was used. The MM5 horizontal domain consisted of a single 36 x 36 km grid with 165 by 129 cells, selected to maximize the coverage of the Eta model analysis region and completely cover the CMAQ modeling domain with some buffer to avoid boundary effects. The MM5 was run on the same map projection as CMAQ. The 2001 meteorological modeling utilized 34 vertical layers with a surface layer of approximately 38 meters. The MM5 and CMAQ vertical structures are shown in Table 5.

Table 5. Vertical layer structure for MM5 and CMAQ (heights are the top of layer).

CMAQ Layers (14)	MM5 Layers (34)	Sigma	Approximate Height (m)	Approximate Pressure (mb)
0	0	1.000	0	1000
1	1	0.995	38	995
2	2	0.990	77	991
	3	0.985	115	987
3	4	0.980	154	982
	5	0.970	232	973
4	6	0.960	310	964
	7	0.950	389	955
5	8	0.940	469	946
	9	0.930	550	937
	10	0.920	631	928
6	11	0.910	712	919
	12	0.900	794	910
	13	0.880	961	892
7	14	0.860	1130	874
	15	0.840	1303	856
	16	0.820	1478	838
8	17	0.800	1657	820
	18	0.770	1930	793
9	19	0.740	2212	766
	20	0.700	2600	730
10	21	0.650	3108	685
	22	0.600	3644	640
11	23	0.550	4212	595
	24	0.500	4816	550
	25	0.450	5461	505
12	26	0.400	6153	460
	27	0.350	6903	415
	28	0.300	7720	370
	29	0.250	8621	325
13	30	0.200	9625	280
	31	0.150	10764	235
	32	0.100	12085	190
	33	0.050	13670	145
14	34	0.000	15674	100

A complete description of the configuration and evaluation of the 2001 meteorological modeling is contained in McNally (2003), however some of the key model physics options are as follows:

- Cumulus Parameterization: Kain-Fritsch
- Planetary Boundary Layer Scheme: Pleim-Chang
- Explicit Moisture Scheme: Reisner 2

- Radiation Scheme: RRTM longwave scheme
- Land Surface Model: Pleim-Xiu
- Four-Dimensional Data Assimilation (FDDA): analysis nudging only

The annual MM5 simulation was divided into four separate periods: 12/16/00 to 4/05/01, 3/16/01 to 7/05/01, 6/14/01 to 10/02/01, and 9/17/01 to 2/04/02. Within each of these periods the model was run for 5 ½ days blocks with a restart occurring at 1200 UTC every fifth day. To assure continuity in the surface moisture, the model initial conditions were updated with the soil conditions from the end of the previous 5 ½ day period using the EPA “INTERPX” processor.

In terms of the 2001 MM5 model performance evaluation, we used an approach which included a combination of qualitative and quantitative analyses to assess the adequacy of the MM5 simulated fields. The qualitative aspects involved comparisons of the model estimated sea level pressure and radar reflectivity fields against observed values of the same parameters from historical weather chart archives. The statistical portion of the evaluation examined the model bias and error for temperature, water vapor mixing ratio, and the index of agreement for the wind fields. These statistical values were calculated on a regional basis. The results of the evaluation indicate that the 2001 model data had a bias in surface temperature of -0.6 degrees Celsius and the error averaged 2.1 degrees C. The humidity fields had a bias of -0.2 g/kg and an error of 1.0 g/kg. The wind speed index of agreement averaged 0.86. The model was found to overestimate precipitation, on average by about 1.6 cm. The precipitation bias was strongest in the summer. Qualitatively, the model fields closely matched the observed synoptic patterns, which is expected given the use of FDDA. In general, the bias and error values associated with the 2001 data are in the range of model performance found from other non-EPA regional meteorological model applications (Environ, 2001).

The MM5 outputs were processed to create model-ready inputs for CMAQ using the Meteorology-Chemistry Interface Processor (MCIP) as described in EPA (1999b). MCIP version 2.2gvm was used to convert the MM5 output to CMAQ meteorological input. This version contained two differences from the main MCIP version 2.2 in that: 1) it allowed for treatment of the graupel associated with the Reisner 2 microphysics scheme and 2) it included a patch to compensate for a minor error in MM5 associated with vegetation fractions.

D. Initial and Boundary Condition Inputs to CMAQ

In this section we describe the approach used to provide the boundary conditions (BCs) and the concentrations used to initialize the model runs for the CAMR CMAQ modeling. Non-episodic national modeling, such as the CAMR annual mercury modeling, requires the prescription of BC's to account for the influx of pollutants and precursors from the upwind source areas outside the modeling domain. The pollutant influxes from the upwind boundaries, which are often dynamic in nature, can affect pollutant concentrations within the modeling domain. For example, a number of recent studies show that long-range, intercontinental transport of pollutants is important for simulating seasonal/annual ozone, PM and mercury (Jacob, et al., 1999; Jaffe et al., 2003; Fiore, et al., 2003, Selin 2005). A scientifically sound approach to estimate incoming pollutant concentrations associated with intercontinental transport

is to use a global chemistry model to provide dynamic BCs for the regional model simulations.

For the CAMR annual mercury modeling, we used the predictions from a global three-dimensional chemistry model, the GEOS-CHEM model (Yantosca, 2004), to provide the BCs and initial concentrations. The global GEOS-CHEM model simulates atmospheric chemical and physical processes driven by assimilated meteorological observations from the NASA's Goddard Earth Observing System (GEOS). This model was run for 2001 with a grid resolution of 2 degree x 2.5 degree (latitude-longitude) and 20 vertical layers. The predictions were used to provide one-way dynamic BCs at 3-hour intervals and initial concentration field for the CMAQ simulations. We used an interface utility tool developed at the University of Houston (Byun and Moon, 2004; Moon and Byun, 2004) to link the GEOS-CHEM with CMAQ. The scale, chemical, and dynamic linking between the two models are needed since the horizontal and vertical coordinates, chemical species representations, and model output time are different. A detailed description of how the GEOS-CHEM model outputs were used to develop inputs to CMAQ including the data preparation, spatial and temporal conversion procedures, and species mapping tables are given in Moon and Byun (2004).

E. CMAQ Model Applications

For CAMR, CMAQ was run for six emissions scenarios: a 2001 base year, a 2001 base year with utility mercury emissions zeroed-out, a 2020 projection with CAR incorporated, a 2020 projection with CAR incorporated and utility mercury emissions zeroed-out, a 2020 projection with CAR and CAMR control option 1 incorporated, and a 2020 projection with CAR and CAMR control option 2 incorporated.

IV. CMAQ Model Performance Evaluation

At this point in time, it is difficult to assess model performance for total mercury deposition. Scientist currently believe through analysis of very limited measurements that wet and dry deposition are approximately equal in magnitude. There currently is no measurement network to evaluate the performance of models in estimating dry deposition of mercury. Thus, we are not able to evaluate the performance of air quality models in predicting dry deposition, which is thought to be roughly half of total mercury deposition. There is a network of mercury wet deposition monitors, which are scattered throughout remote locations in the United States and Canada, mostly in the east. Thus, model predictions of wet deposition can be evaluated by a monitoring network.

An operational model performance evaluation for mercury wet deposition for 2001 was performed to estimate the ability of the CMAQ modeling system to replicate base-year wet depositions of mercury. The wet deposition evaluation principally comprises statistical assessments of model versus observed pairs that were matched in time and space on a seasonal and annual basis. The statistics are presented separately for the entire domain, the East, and the West (using the 100th meridian to divide the eastern and western United States).

A. Performance Statistical Definition

Below are the definitions of statistics used for the evaluation. The statistics are similar to those used for a previous evaluation (Wayland, 1999). The format of all the statistics is such that negative values indicate model predictions that were less than their observed counterparts. Positive statistics indicate model overestimation of observed counterparts.

Mean Observation: The mean observed mercury wet deposition (ug/m^2) averaged over all monitored weeks in the year and then averaged over all sites in the region.

$$OBS = \frac{1}{N} \sum_{i=1}^N Obs_{x,t}^i$$

where: N = the number of measurement sites

Obs = observed deposition at monitoring site x over time t (i.e., Annual)

Mean Prediction: The mean model predicted mercury wet deposition (ug/m^2) paired in time and space with the observations and then averaged over all sites in the region.

$$PRED = \frac{1}{N} \sum_{i=1}^N Pred_{x,t}^i$$

where: N = the number of measurement sites

Pred = model predicted deposition at monitoring site x over time t (i.e., Annual)

Ratio of the Means: Ratio of the predicted over the observed values. A ratio of greater than 1 indicates on overprediction and a ratio of less than 1 indicates an underprediction.

$$RATIO = \frac{1}{N} \sum_{i=1}^N \frac{Pred_{x,t}^i}{Obs_{x,t}^i}$$

Mean Bias (ug/m^2): This performance statistic averages the difference (model - observed) over all pairs in which the observed values were greater than zero. A mean bias greater than zero indicates that the model overpredicts and a bias less than zero indicates the model underpredicts. This model performance estimate is used to make statements about the absolute or unnormalized bias in the model simulation.

$$BIAS = \frac{1}{N} \sum_{i=1}^N (Pred_{x,t}^i - Obs_{x,t}^i)$$

Mean Fractional Bias (percent): Normalized bias can become very large when a minimum

threshold is not used. Therefore fractional bias is used as a substitute. The fractional bias for cases with factors of 2 under- and over-prediction are -67 and + 67 percent, respectively. Fractional bias is a useful model performance indicator because it has the advantage of equally weighting positive and negative bias estimates.

$$FBIAS = \frac{2}{N} \sum_{i=1}^N \frac{(Pred_{x,t}^i - Obs_{x,t}^i)}{(Pred_{x,t}^i + Obs_{x,t}^i)} * 100$$

Mean Fractional Error (percent): It is similar to the fractional bias except the absolute value of the difference is used so that the error is always positive.

$$FERROR = \frac{2}{N} \sum_{i=1}^N \frac{|Pred_{x,t}^i - Obs_{x,t}^i|}{Pred_{x,t}^i + Obs_{x,t}^i} * 100$$

B. Results of CMAQ Model Performance Evaluation

For mercury wet deposition, this evaluation includes comparisons of model predictions to the corresponding measurements from the Mercury Deposition Network (MDN). The statistics were calculated using the predicted-observed pairs for the full year of 2001 and for each season, separately. Only sites where data was available more than half the weeks in a season were utilized for the seasonal performance evaluation and only sites that had four seasons meeting this data completeness requirement were utilized for the annual performance evaluation. There were 52 MDN sites in 2001 that meet the annual data completeness requirements, of those sites 48 were located in the east and 4 were located in the west. The results for the annual performance evaluation are shown below in Table 6.

Table 6. CMAQ Performance Statistics for Mercury Wet Deposition: 2001

Area	No. of MDN Sites	Mean CMAQ Predictions (ug/m ²)	Mean Observations (ug/m ²)	Ratio of Means (pred/obs)	Bias (ug/m ²)	Fractional Bias (%)	Fractional Error (%)
Entire Domain	52	7.29	9.46	0.77	-2.17	-23.2	30.2
East	48	7.25	9.79	0.74	-2.55	-27.0	30.2
West	4	7.76	5.41	1.43	2.34	21.7	30.5

The results contained in Table 6 shows that averaged annually over all MDN monitoring sites, CMAQ underestimates mercury wet deposition by approximately 23 percent with an fractional error of approximately 30 percent. The 4 MDN sites in the west do not provide an adequate or representative basis for inferring model performance.

A scatter plot of the observed versus predicted annual mercury wet deposition for all the sites is shown below in Figure 2. It can be seen that although the CMAQ model tends to underpredict mercury wet deposition on average, the majority of predictions are within 30 percent of observed values. Most of the remaining sites have predictions that are within 50 percent of observations. There is one site in the west in British Columbia where the model overpredicts by greater than a factor of 2. However, the precipitation at this site was overpredicted by the meteorological input model by 55 percent.

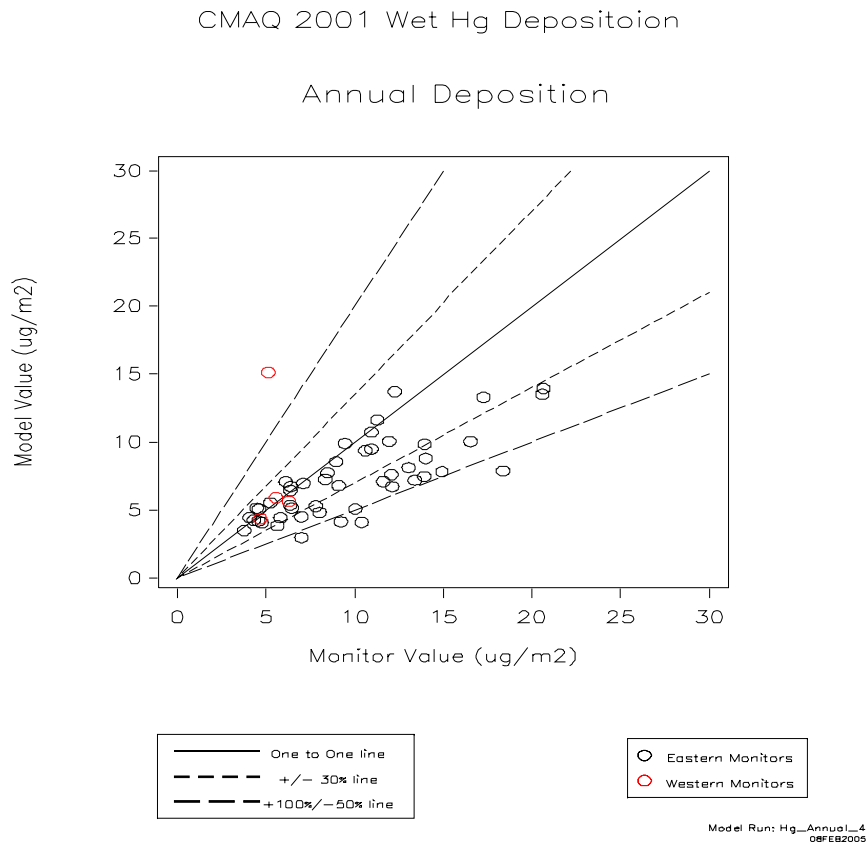


Figure 2. Scatter Plot of Modeled versus Monitored Mercury Wet Deposition: 2001

V. Impacts of CAMR on Mercury Depositions

Section A discusses the results of the mercury deposition modeling for the 2001 base case, 2020 CAR and 2020 CAMR modeling. Section B discusses the potential effects of CAR in 2015 on mercury deposition, although this was not explicitly modeled.

A. Mercury Depositions for 2001 Base Case, 2020 CAR and 2020 CAMR

Maps showing the mercury deposition results are provided below. The annual total modeled mercury deposition for the 2001 base case is shown in Figure 3. The reduction in total mercury deposition that would result if all US power plant mercury emissions were zeroed-out is shown in Figure 4. The change in total mercury deposition in 2020 with CAR relative to 2001 is shown in Figure 5. The annual total mercury deposition for 2020 with CAR is shown in Figure 6. The change in 2020 CAR total mercury depositions with CAMR Option 1 is shown in Figure 7. The change in 2020 CAR total mercury depositions with CAMR Option 2 is shown in Figure 8. It can be seen in Figures 4 and 5 that the implementation of CAR and other minor non-utility mercury emissions decreases in 2020 result in a similar reduction in total mercury deposition as completely eliminating power plant mercury emissions. The main cause of this result is CAR results in a very large decrease in reactive gaseous mercury (RGM) emissions from Power Plants through the implementation of scrubber control technology (see Table 2). RGM is the most readily deposited form of mercury. It can be seen in Figures 7 and 8 that the implementation of CAMR Option 1 and CAMR Option 2 results in some scattered total mercury deposition reductions beyond CAR in 2020, but for the most part these reductions are not very significant compared to those obtained by CAR. Most of the mercury emissions reductions from CAMR are in the form of elemental mercury (Hg0). This form of mercury is not readily deposited, but enters the global pool of mercury. Thus, CAMR will result in a reduction of the transport of mercury to other places in the world.

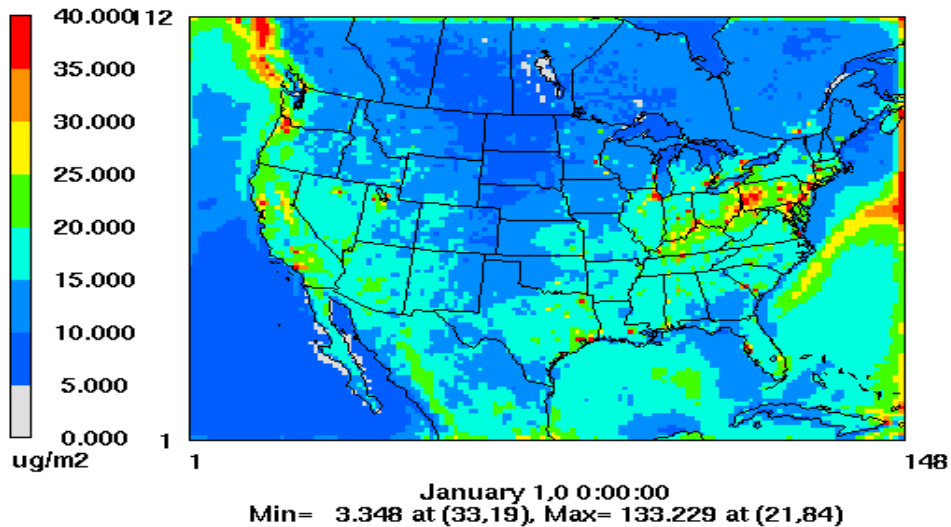


Figure 3. Base Case Total Mercury Deposition: 2001

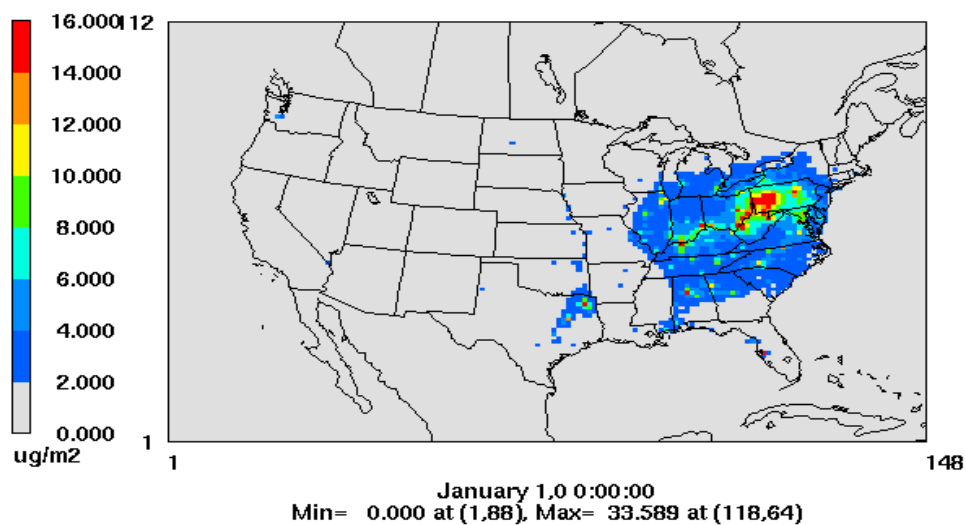


Figure 4.
Decrease in Total Mercury Deposition with Power Plant Zero-Out Simulation: 2001

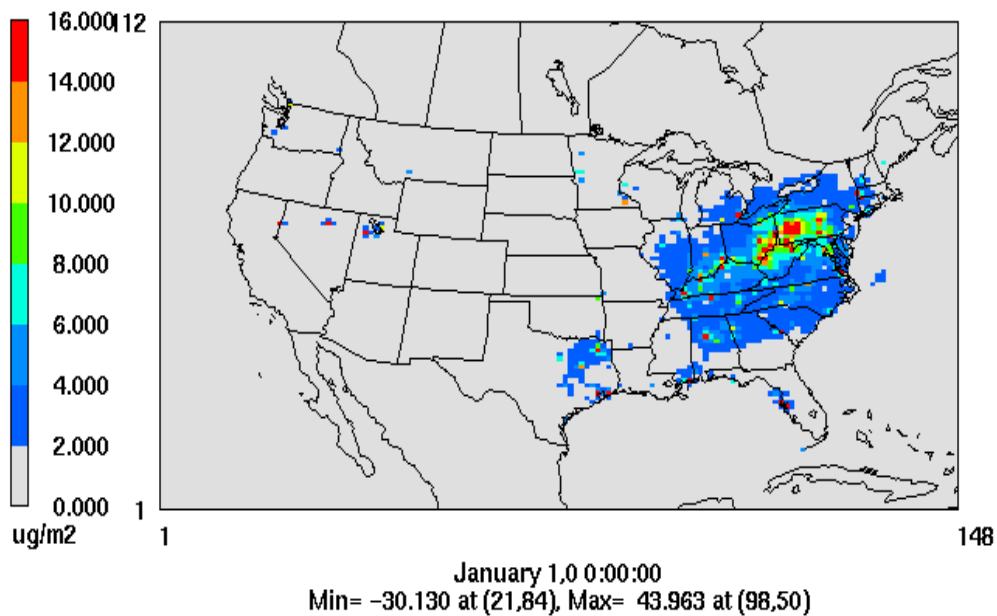


Figure 5. ***Change in Total Mercury Deposition for all Sources: 2020 with CAR Relative to 2001***

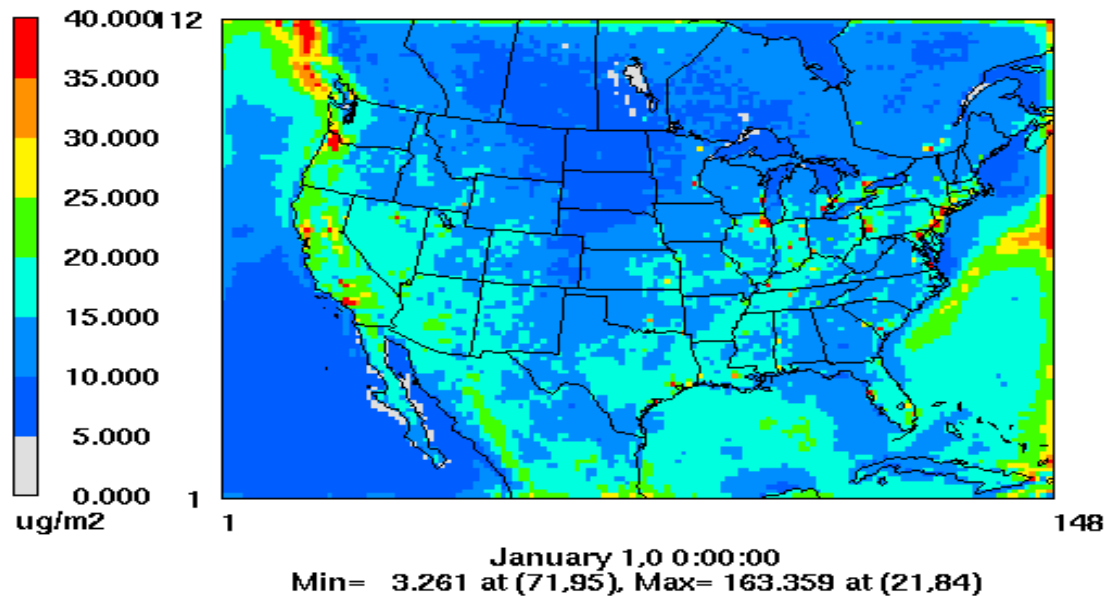


Figure 6. Total Mercury Deposition: 2020 with CAR

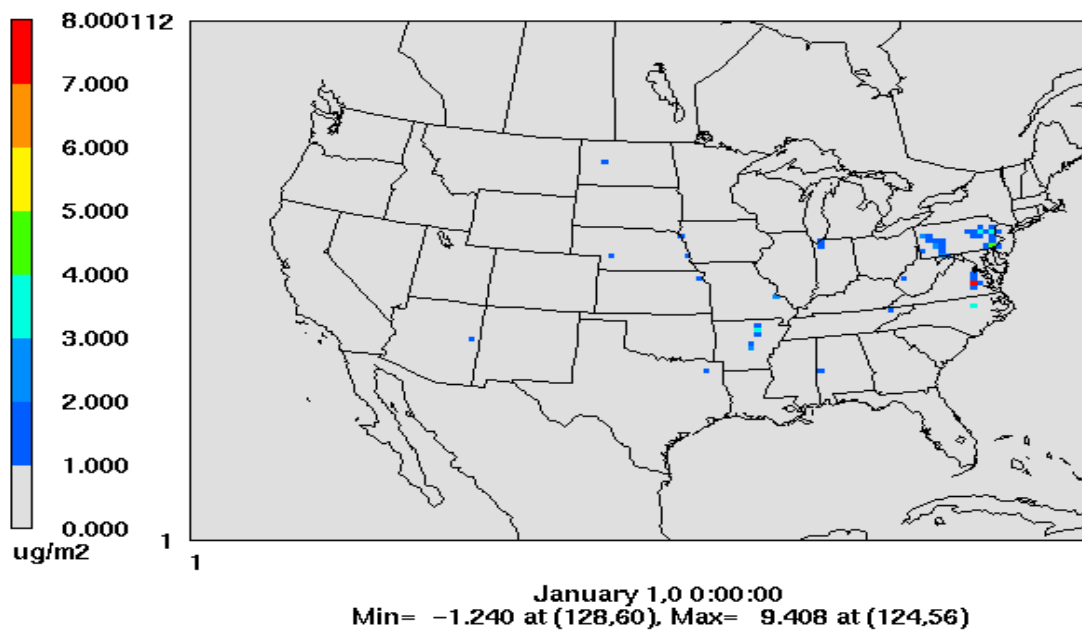


Figure 7. Change in Mercury Depositions from Power Plants Due to CAMR Option 1: 2020

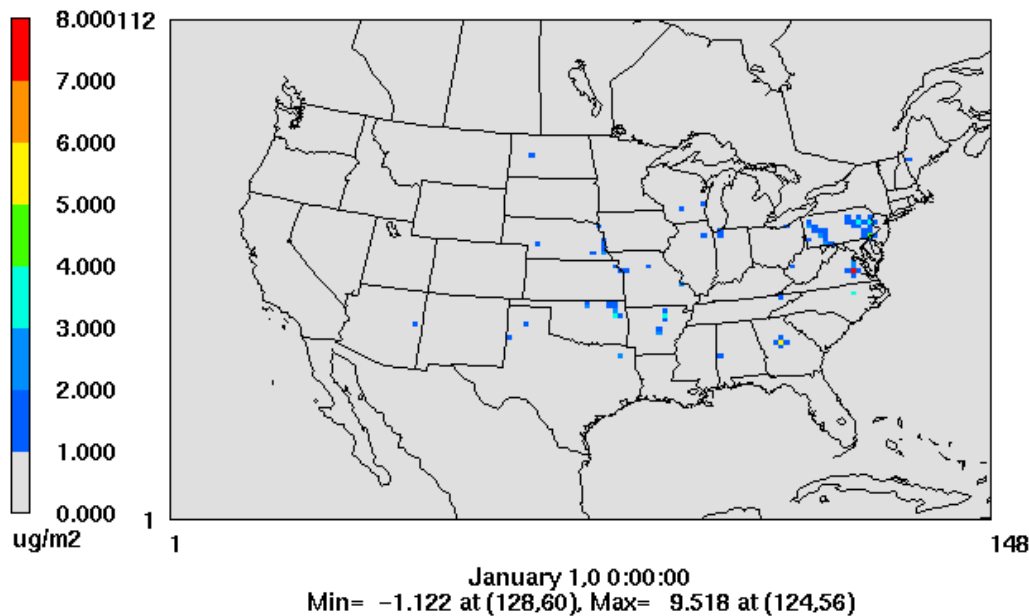


Figure 8. Change in Mercury Depositions from Power Plants Due to CAMR Option 2: 2020

B. Mercury Deposition in 2015 with CAR

Although EPA did not directly model the effects of CAR on mercury deposition in 2015, the impacts are not expected to differ too much from the modeling for the 2020 baseline with CAR. The estimated total mercury emissions of just over 34 tons from EGUs in 2015 with CAR will be virtually the same as the estimated total in 2020 with CAR. The readily deposited non-elemental mercury emissions from EGUs are estimated to be 10 tons in 2015 but roughly 9 tons in 2020. The non-elemental mercury emissions consists of the sum of the reactive gaseous mercury and particulate mercury species. It could be inferred that although 2015 was not modeled here that the mercury deposition levels that are estimated to occur with CAR in 2020 as shown in Figure 6 are similar to those that would occur in 2015 with CAR. Thus, the difference in mercury deposition from 2001 to CAR in 2020 as shown in Figure 7 should also be indicative of the change between 2001 and CAR in 2015.

The similarity between these scenarios will depend upon the following three factors:

- 1) The levels of criteria pollutant emissions are different across these years and would effect the mercury deposition through the atmospheric reactions accounted for by CMAQ. However, the potential for these interactions to cause notable differences is limited as the emissions differences are not significant enough for these interactions to be more than a second-order impact.
- 2) The spatial distribution of mercury emissions reductions in emissions across these years will

influence the spatial nature of mercury deposition. Despite the fact that the level of total mercury emissions is virtually the same for both years, the spatial distribution of these emissions reductions across EGUs will likely differ between 2015 and 2020. This difference should lead to the spatial coverage of reductions in mercury deposition to be somewhat less in 2015 than 2020 similar to the reduced spatial coverage observed in the modeling for the 2020 baseline with CAR compared to 2020 CAMR options.

3) The level of mercury emissions reductions by species across these years would effect the modeled levels of mercury deposition. Despite the fact that the level of total mercury emissions is virtually the same for both years, the more readily deposited non-elemental emissions are different by roughly 10 percent, or 10 vs 9 tons respectfully for 2015 and 2020. This difference should also contribute to a lessening of the spatial coverage of mercury deposition reductions in 2015 than 2020. The mercury emissions from sectors other than EGUs are also expected to differ between these years. In addition to the spatial differences, these differences in emissions will contribute to an undetermined difference in the spatial coverage of mercury deposition reductions in 2015 than 2020.

VI. Summary of Findings: HUC Level Deposition Analysis

The cumulative distribution of Hydrologic Unit Code (HUC) level depositions across watersheds are provided in Table 7 and Figure 9. The cumulative percentage of HUCs that have deposition less than the value on the x-axis for each of the six modeled scenarios are shown in Figure 9. For example, 90 percent of the HUCs have depositions below 22.16 ug/m² in the 2001 base case. For the 2020 CAR plus CAMR Option 1 scenario, 90 percent of the HUCs have depositions below 19.48 ug/m².

Table 7. Summary Statistics of Total Mercury Depositions (ug/m²) by Modeling Scenario

	2001 Base Case	2001 Utility Hg Zero-Out	2020 CAR	2020 Utility Hg Zero-Out	2020 CAR & CAMR Option 1	2020 CAR & CAMR Option 2
Minimum	6.994	6.942	6.078	5.898	6.075	6.075
Maximum	54.54	54.38	62.76	62.72	62.76	62.75
50 th percentile	15.92	14.60	14.59	13.92	14.44	14.39
90 th percentile	22.16	19.48	19.46	19.04	19.37	19.33
99 th percentile	32.35	27.20	29.15	28.93	28.96	28.95

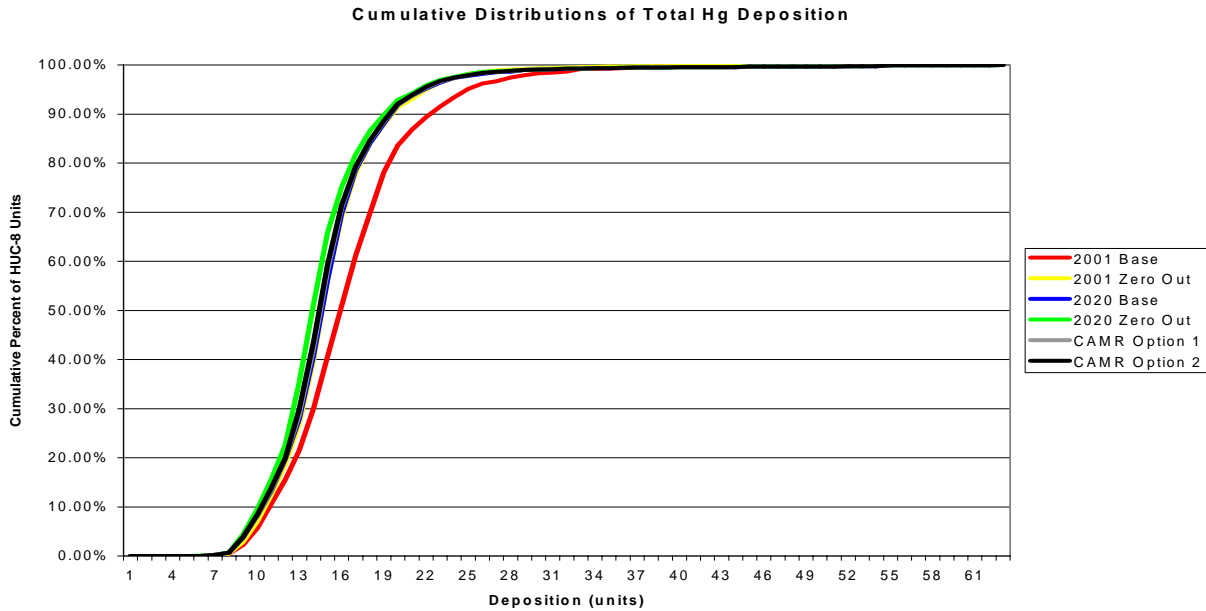


Figure 9. Cumulative Distribution of Total Mercury Deposition ($\mu\text{g}/\text{m}^2$) at HUC-8 Level by Modeling Scenario

The cumulative distribution of Hydrologic Unit Code (HUC) level depositions attributable to utilities are provided in Table 8 and Figure 10. The cumulative percentage of HUCs that have deposition less than the value on the x-axis for 4 of the modeled scenarios are shown in Figure 10. For example, 90 percent of the HUCs have depositions attributable to utilities below $4.08 \mu\text{g}/\text{m}^2$ in the 2001 base case. For the 2020 CAR plus CAMR Option 1 scenario, 90 percent of the HUCs have depositions attributable to utilities below $1.16 \mu\text{g}/\text{m}^2$. CAR shifts the distribution of utility attributable deposition significantly, resulting in a 75 percent reduction in the 99th percentile of utility attributable deposition, and a 20 percent reduction in the 50th percentile. CAMR Option 1 and Option 2 results in an additional reduction in 2020 utility attributable deposition in the 99th percentile of 15 and 20 percent, respectively. At the 50th percentile, CAMR Option 1 and Option 2 result in an additional reduction of 2020 utility attributable deposition of 16 and 29 percent, respectively. As can be seen in Figure 11, CAR also shifts the distribution of percentage of HUCs with deposition attributable to utilities. In the 2001 base case, 10 percent of HUCs had greater than 20 percent of deposition attributable to utilities. In the 2020 with CAR scenario, 10 percent of HUCs had greater than 10 percent of deposition attributable to utilities. In the 2020 CAR plus CAMR Option 1 scenario, 10 percent of HUCs had greater than 7 percent of deposition attributable to utilities.

Table 8. Utility Attributable Deposition ($\mu\text{g}/\text{m}^2$) Statistics

Statistics	2001 Base Case	2020 CAR	2020 CAR & CAMR Option 1	2020 CAR & CAMR Option 2
Minimum	0.00	0.00	0.00	0.00
Maximum	19.71	4.03	3.85	3.80
50 th percentile	0.39	0.31	0.26	0.22
90 th percentile	4.08	1.38	1.16	0.99
99 th percentile	10.15	2.56	2.17	2.04

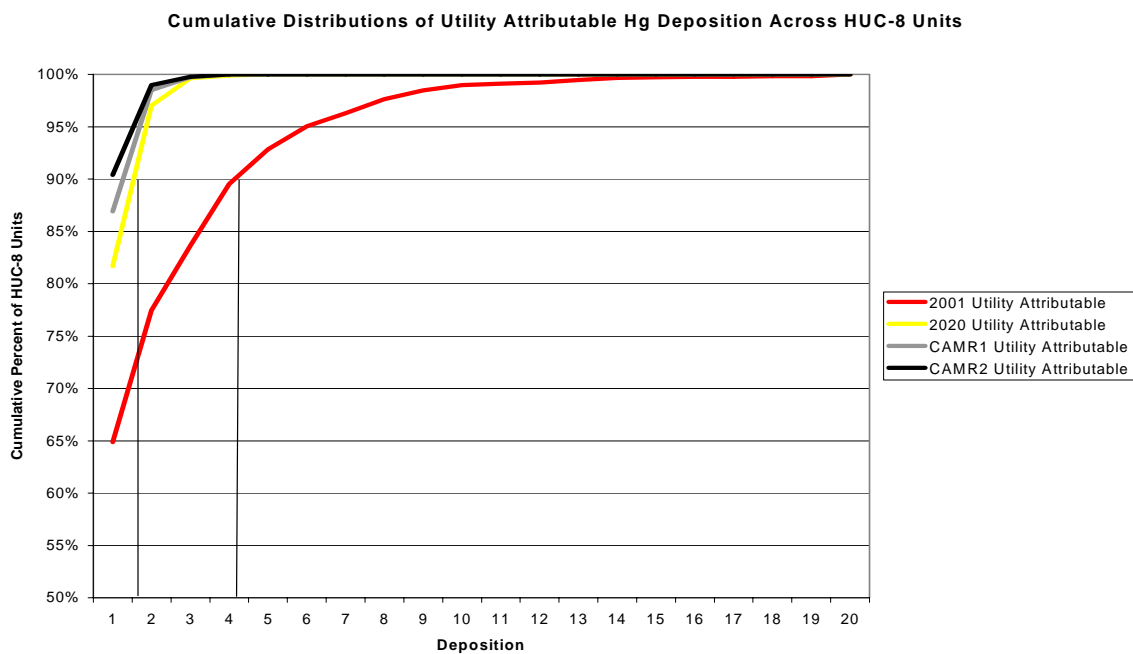


Figure 10. Cumulative Distribution of Utility Attributable Mercury Deposition ($\mu\text{g}/\text{m}^2$) at HUC-8 Level by Modeling Scenario

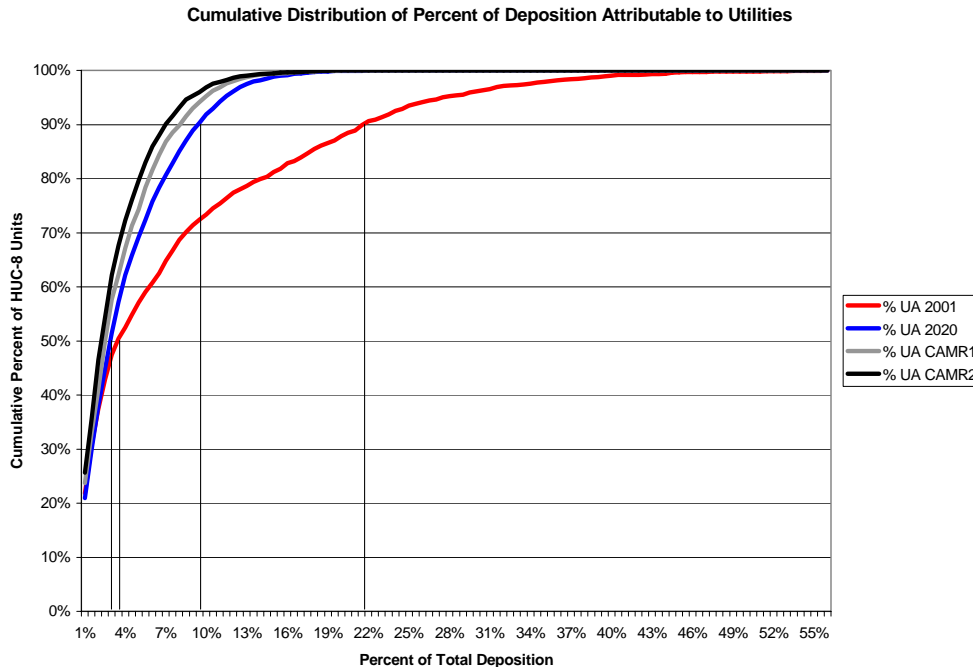


Figure 11. Cumulative Distribution of Percent Deposition Attributable to Utilities at HUC-8 Level by Modeling Scenario

II. References

Bullock, R. and Brehme, K., “Atmospheric Mercury Simulation Using the CMAQ Model: Formulation, Description, and Analysis of Wet Deposition Results,” *Atmospheric Environment* 36, 2135-2146, 2002.

Byun, D.W., and Ching, J.K.S., Eds, 1999. *Science algorithms of EPA Models-3 Community Multiscale Air Quality (CMAQ modeling system, EPA/600/R-99/030, Office of Research and Development, U.S. Environmental Protection Agency.*

Byun D.W., N.K.Moon, Daniel Jacob, and Rokjin Park, “Regional Transport Study of Air Pollutants with Linked Global Tropospheric Chemistry and Regional Air Quality Models,” 2nd ICAP workshop, RTP, NC, October 2004, http://www.cep.unc.edu/empd/projects/ICAP/2004wkshp_pres.html.

Byun, D.W., and Schere, K.L., 2004. Review of the Governing Equations, Computational Algorithms, and Other Components of the Models-3 community Multiscale Air Quality (CMAQ) Modeling System. *J. Applied Mechanics Reviews*, XX, ps. XX

Dennis, R.L., Byun, D.W., Novak, J.H., Galluppi, K.J., Coats, C.J., and Vouk, M.A., 1996. The next generation of integrated air quality modeling: EPA’s Models-3, *Atmospheric Environment*, 30, 1925-1938.

Environ, Enhanced Meteorological Modeling and Performance Evaluation for Two Texas Episodes. August 2001.

EPA, 1999b. Science Algorithms of the EPA MODELS-3 Community Multiscale Air Quality (CMAQ) Modeling System, EPA/600/R-99/030, March 1999.

EPA, 2005a. Clean Air Mercury Rule Emission Inventory Technical Support Document. Office of Air Quality Planning and Standards. Research Triangle Park, NC.

EPA, 2005b. Updated CMAQ Model Performance Evaluation for the 2001 Annual Simulation, Office of Air Quality Planning and Standard, Research Triangle Park, NC.

Fiore, A.M., D.J. Jacob, H. Liu, R.M. Yantosca, T.D. Fairlie, and Q. Li, "Variability in surface ozone background over the United States: Implications for air quality policy," *J. Geophys. Res.*, 108, 4787, 2003.

Grell, G., J. Dudhia, and D. Stauffer, 1994: A Description of the Fifth-Generation Penn State/NCAR Mesoscale Model (MM5), NCAIR/TN-398+STR., 138 pp, National Center for Atmospheric Research, Boulder CO.

Jacob, D.J., J.A. Logan, and P.P. Murti, "Effect of Rising Asian Emissions on Surface Ozone in the United States," *Geophys. Res. Lett.*, 26, 2175-2178, 1999.

Jaffe D., McKendry I., Anderson T., and Price H. "Six 'new' episodes of trans-Pacific transport of air pollutants," *Atmos. Envir.* 37, 391-404, 2003.

McNally, D, Annual Application of MM5 for Calendar Year 2001, Topical report submitted to EPA, March 2003.

Moon N.K., and D.W. Byun, "A Simple User's Guide for "geos2cmaq" Code: Linking CMAQ with GEOS-CHEM, Version 1.0," Interim Report from Institute for Multidimensional Air Quality Studies (IMAQS), University of Houston, TX, August 2004, <http://www.math.uh.edu/~dwbyun/Meetings/icap/>.

Selin, N.E., "Mercury Rising: Is Global Action Needed to Protect Human Health and the Environment?", *Environment* 47, 22-35, February 2005.

Wayland, R.J., 1999. REMSAD- 1990 Base Case Simulation: Model Performance evaluation- Annual Average statistics, Office of Air Quality Planning and Standards, Research Triangle Park, NC.

Yantosca, B., 2004. GEOS-CHEMv7-01-02 User's Guide, Atmospheric Chemistry Modeling Group, Harvard University, Cambridge, MA, October 15, 2004